Passive Maritime Surveillance Using Satellite Communication Signals

ANDREW G. STOVE, Senior Member, IEEE
MARINA S. GASHINOVA
STANISLAV HRISTOV
MIKHAIL CHERNIAKOV
University of Birmingham, Birmingham, U.K.

In this paper, the feasibility of a bistatic passive system for maritime surveillance and marine navigation is considered based on the communication satellite constellation Inmarsat as a source of illuminating signals. A power budget analysis is detailed for Inmarsat signals, considering both the reference and the radar channels. The effect of sea clutter is also examined. It is shown that relatively poor range resolution can be improved if the available communication channels are combined to improve the bandwidth, a process that also improves the sensitivity. For the first time, detection and preliminary bistatic range-Doppler tracking are presented for a representative maritime target.

Manuscript received September 15, 2016; revised April 25, 2017; released for publication May 30, 2017. Date of publication August 2, 2017; date of current version December 5, 2017.

DOI. No. 10.1109/TAES.2017.2722598

Refereeing of this contribution was handled by R. M. Narayanan.

Authors' address: A. G. Stove, M. S. Gashinova, S. Hristov, and M. Cherniakov are with the School of Electronic, Electrical and Systems Engineering, University of Birmingham, Birmingham B15 2TT, U.K., E-mail: (a.stove@bham.ac.uk; m.s.gashinova@bham.ac.uk; s.z.hristov@bham.ac.uk; m.cherniakov@bham.ac.uk. *(Corresponding author: Stanislav Hristov.)*

I. INTRODUCTION

The last decade has seen a surge of passive radar research, using a wide variety of potential illuminators [25]. Passive radar systems have been proposed for the detection and tracking of ground, maritime, or airborne targets, in most cases using terrestrial broadcasting signals [2]–[6]. Passive systems represent an alternative way to provide large-area surveillance with persistent monitoring with a low environment impact and low cost without incurring the overheads and delays needed to introduce a new "primary" system. The choice of terrestrial broadcasting systems as Illuminators of Opportunity (IoO's) is dictated by their accessibility, large transmitted powers, excellent coverage at least in populated areas, and reasonably large bandwidth providing acceptable range resolution, making them a perfect candidate for the ubiquitous surveillance network.

However, limited earth coverage and the potential vulnerability of terrestrial broadcasters in situation of man-made or natural disasters limit their universality and reliability and therefore reduce their attractiveness of such systems for pervasive surveillance.

Instead, spaceborne IoO's may help to tackle such restrictions.

In military applications, its passive nature will make interception and electronic attack much harder or even impractical. At shorter ranges, the effects of glint on the tracking accuracy will be reduced because: 1) the bistatic radar cross section (RCS) is not much affected as the monostatic RCS by specular reflectors and 2) presumably lower operational frequencies of transmitters of opportunity than that of the traditional dedicated system. Therefore, there is a need to analyze the suitability of available systems and to discuss the optimum tradeoff of parameters that can deliver the required performance.

The goal of this paper is, therefore, to investigate the performance of bistatic passive system for the detection and kinematic parameters estimation of maritime targets.

II. ANALYSIS OF PROSPECTIVE TRANSMITTERS OF OPPORTUNITY

To provide the required sensitivity for detecting targets of interest, the prospective IoO should be considered in terms of

1) transmit power;
2) carrier frequency;
3) illuminating signal bandwidth; and
4) number of the transmitters visible simultaneously.

For the complete system design, there are, of course, also other parameters that are important, such as

1) spatial availability;
2) knowledge of transmitter position;
3) availability over time (pervasiveness);
4) ownership of the transmitters; and
5) vulnerability of the transmitter;

The significance of these factors will be made clear below.

A. Factors Influencing Detection Performance

1) *Transmit Power:* The power flux density (PFD) produced by the transmitter in areas of interest must be adequate to provide the required signal-to-noise (SNR) at the receiver for the signals reflected from the targets of interest at the distances defined by the application.

2) *Carrier Frequency:* The transmit signal carrier frequency is a relatively soft requirement, though certain aspects need to be considered. Utilization of signals from different independent IoO operating within the same RF band will lead to the simplicity of the multifunctional receiver that can provide multiaspect observation, more accurate positioning, and higher reliability of the system. This favors L-band operation, with the additional advantage of lower atmospheric attenuation and fading in comparison with high frequency signals, such as Ka band.

3) *Illuminating Signal Bandwidth:* The bandwidth of the signals defines the radar range resolution, a parameter that defines the system performance in multitarget scenarios and reduces its sensitivity to surface or volume clutter.

4) *Number of the Transmitters Visible Simultaneously:* The reliability of the system is totally dependent on the availability of the IoO and, obviously, the more the transmitters are simultaneously visible, the less is the chance of system failure due to signal outage. In addition, in bistatic systems the care should be taken to avoid unfavorable bistatic geometries, such as forward scatter, and, therefore, spatial diversity of multiple IoOs provides the opportunity to choose the best configuration. Moreover, powers from several transmitters could be at least noncoherently combined to improve the system performance.

B. Factors Affecting System Performance

1) *Spatial Availability:* The "spatial availability" is a way of expressing which areas are covered by the transmitter. For maritime surveillance, global coverage is needed, although this requirement can be relaxed to exclude areas around the geographical poles. In this respect, global navigation satellite system (GNSS) systems and Iridium are ideal, the communications systems in geostationary earth orbit (GEO) give global coverage up to latitudes of about 80°, whereas broadcast transmitters are only designed to give coverage over land and littoral regions, not over the open sea.

2) *Knowledge of Transmitter Position:* The position in space of the transmitter must be well characterized in order to be able to estimate the target position and velocity.

3) *Availability Over Time (Pervasiveness):* The temporal availability characterizes the proportion of time for which a suitable IoO is present. The signal of opportunity is required to be available at any time, day or night, on any day.

4) *Ownership of the Transmitters:* Transmitters that are owned by a commercial organization or by national governments may be switched OFF or their parameters are changed, which may degrade the signal's suitability as an IoO. This may be done deliberately to disrupt a passive coherent location (PCL) system "hitchhiking" on it.

This factor is directly related to the system reliability and pervasiveness. Ideally, transmitters would belong to international organization or allies' defense or national institutions. This would prevent global denying access to the signals.

5) *Vulnerability of the Transmitter:* A transmitter that is vulnerable in the event of man-made or natural catastrophes would not be suitable for a reliable, pervasive system. Spaceborne systems are very robust to events on the earth's surface. But the broadcasting organizations also take a lot of effort to ensure that their transmission infrastructure is very robust.

From the perspective of target detection, satellite-based transmitters could be viewed as the most suitable. Significant emitters are the Inmarsat I-4 and Iridium communication satellites and the uprated GPS and the Galileo satellite navigation systems. From the perspective of the "system" issues, all three emitter types are suitable as seen in Table I.

While GNSS satellites provide global coverage their PFD at the earth is about 30–40 dB less than that of communication satellites [1]. A combination of signals may improve the power budget. To work as a navigation system, a GNSS system must provide at least four satellites in sight at any time. In practice, there will typically be six in sight. The rule of thumb given in Section III.G indicates that the incoherent integration of these multiple signals will give an extra gain of about 6 dB. This extra gain is not, however, sufficient to overcome the problems of the limited flux density, therefore, in spite of the attractive bandwidth and spatial/temporal availability, current accessible GNSS signals are not suitable for the remote detection of marine targets.

In its turn, the communication satellites with allegedly global or near global coverage, such as Inmarsat and Iridium, may provide satisfactory PFD, but they are less attractive in terms of the bandwidth and pervasiveness and, therefore, the research should be focused on the development of approaches to improve the resolution and to investigate if multimode operation, i.e., various combinations of different IoO, services, channels etc., can enhance the system performance.

It is noticeable that Inmarsat-4 and Iridium provide similar "headline" power densities of -66 and -70 dBm/m^2 at the earth's surface, respectively, despite their very different orbital heights—about 36 000 km (GEO) for Inmarsat and 780 km for Iridium (LEO)—because they both need sufficient power density to send down useful data rates into receivers with modest antenna apertures. The wider bandwidth of Inmarsat is matched by the fact that its receivers use antennas with an area typically of the order of 0.1 m^2, whereas those used by Iridium, with its lower data rate, appear to be essentially monopoles.

Both of these systems operate in "L" band. The systems operate at slightly different frequencies, but the difference between them is, again, not significant given the other

TABLE I
Characteristics of Prospective Satellite Systems as IoO's

Parameter	GNSS (GPS, GLONAS, Galileo)	Mobile Satellite Communication	Satellite Broadcasting
Transmit power	Marginal to low	Medium to marginal [2]	High to medium
PFD at the earth surface	Low (-104 dBm/m^2 for GPS; -100 dBm/m^2 for Galileo)	Medium (-66 dBm/m^2 Inmarsat, -70 dBm/m^2 Iridium)	
Transmit signal bandwidth	Medium to high (0.5–10 MHz)	Low (i.e., 31.5 kHz Iridium single channel) to Medium (i.e., 200 kHz Inmarsat single channel), potentially could be combined.	Medium (per channel) potentially could be combined till high
Frequency band	L	L	S or X
Number of the satellites in view	~24	1–5	≈1–2 covering any geographical region

approximations within the modeling, so all the modeling can use the same nominal frequency of 1.5 GHz (20 cm wavelength).

C. Flux Density Available From the Inmarsat System

It should be noted that although [2] quotes a flux density of -64 dBm/m^2 at the earth's surface, this is based on a slightly misleading definition of the effective radiated power. In [7], the total EIRP of the satellite is 67 dBW, but this is the total emitted power multiplied by the gain of each "spot" beam. The space-to-ground links use the spectrum between 1525 and 1559 MHz [8] so the system has approximately 120 channels. This is compatible with the statement given in [7] that the saturation power per link per beam is 55 dBW. This would give a flux density of about -78 dBm/m^2 at the earth's surface.

A single spot on the earth can, however, be illuminated by a number of beams, allowing a number of ground stations in the same region to use the system simultaneously. Each geographical region sees only about one seventh of these channels (i.e., up to about 17 channels) because a degree of frequency diversity is used to prevent different signals from using the same channel at the edge of a "spot." This means that while a radar could potentially use the power from 17 channels, giving a total potential flux density of about -66 dBm/m^2, in practice, as will be shown later, the system will generally see only about 4 channels operating at maximum power.

It can, therefore, be seen that for marine applications, which require illumination over the open sea and a relatively high power density to obtain good detection range, satellite communications systems seem one of the most promising IoO and well worth further investigation, in particular to quantify and verify the expected sensitivity.

In the following section, we start with the analysis of the power budget for Inmarsat transmitters and typical targets.

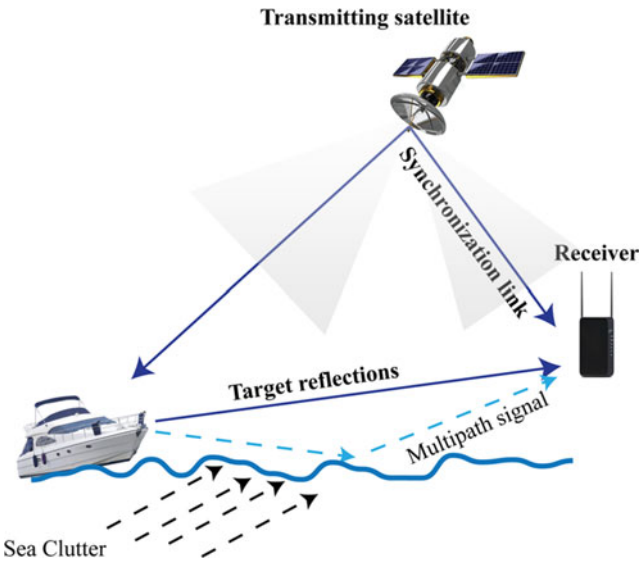

Fig. 1. Passive target detection by PCL consisting of low-altitude receiver and spaceborne transmitter

III. POWER BUDGET ANALYSIS

Fig. 1 shows the general topology of the system where the double channel receiver, which is mounted on either low altitude or seaborne platform, is used to collect reflected signals from a vessel coherently with reference signal—or synchronization signal—from a satellite.

A. Maritime Obstacle Avoidance

Although the primary intention of this paper is to introduce the general concept of the passive maritime radar using satellite communication signals, it is useful to focus on one specific application when discussing the power budget.

Although this concept could have many potential applications, both civil and military, we will consider here a simple marine collision avoidance system. This is a less capable alternative to a navigation radar that would look ahead of a small ship to warn specifically of objects in its

path, in a function more akin to an automotive radar than to a conventional marine radar. A low-cost radar with this capability would be an attractive sensor for small autonomous boats. It would be appropriate as a "baseline" performance for such a system to consider the earlier generation International Maritime Organization requirement for marine radars [9], i.e., the ability to detect a target with an RCS of 10 m^2 at a height of 3.5 m above the sea and at a range of 2 nautical miles.

The experimental results that will be presented in Section V were obtained with the radar on the shore, to avoid the need, for these first experiments, to build hardware that could cope with the marine environment. The results shown are, therefore, more to a shore-based harbor surveillance radar. Note, however, that many such systems are in fact based on marine navigation radars so the results are still able to verify the calculations made here using marine obstacle avoidance as our "straw man" application for the initial exploration of the capabilities of the system.

B. Scenario

The bistatic scattering from a target of approximately 10 m^2 RCS will thus be considered in the sensitivity evaluations as a reference model for radar channel signal estimations, whereas for the synchronization channel the free-space propagation model will be used.

The Inmarsat-4 system will be considered as the illuminator and the signal is considered to consist of four frequency channels each with a bandwidth of 200 kHz and a flux density of -78 dBm/m^2.

The presence of the sea surface in the scenario will give rise both to returns from the sea clutter and to multipath interference, which will affect the strength of the return from the target.

C. Propagation Models for Estimation of Received Power

1) *"Rough Surface" Limit:* The simplest case for modeling occurs in high sea states at the relatively short ranges, where the multipath will not have such a strong effect because the scattering from the sea surface will cease to be specular. In that case, a free-space propagation model can be applied for the estimation of the received power along the path from the target to the receiver:

$$P_{\mathrm{Rx}}^{\mathrm{FS}} = \frac{P_{\mathrm{Target}}}{4\pi d^2} A_{\mathrm{Rx}} \tag{1}$$

where $P_{\mathrm{Target}} = P_{FD} \cdot \sigma$ is a product of PFD near the target produced by a satellite, PFD, and the target bistatic radar cross section σ, d is the receiver-to-target range, and ARx is the effective area of the receive antenna.

2) *"Two Ray" Limit:* However, at low sea states when the sea can be treated as being smooth, the reflection from the sea can be considered to be perfect and the two ray propagation model [10] can be used to predict rapid attenuation of the signal proportional to the fourth power of distance:

$$P_{\mathrm{Rx}}^{\mathrm{Multipath}} \overset{d \gg h_t, h_{\mathrm{Rx}}}{\approx} \frac{4\pi\, P_{\mathrm{Target}} A_{\mathrm{Rx}} {h_t}^2 {h_{\mathrm{Rx}}}^2}{\lambda^2 d^4} \tag{2}$$

where λ is the wavelength of the transmitted signal, h_t and hRx are the height of the target and the elevation of the receiver, respectively.When the path difference between the direct and indirect paths is relatively small, the received power will oscillate with a range around that predicted by the free-space model according to

$$P_{\mathrm{Rx}}^{\mathrm{Multipath}} = \frac{P_{\mathrm{Target}} A_{\mathrm{Rx}}}{4\pi d^2} 4 \cdot \sin^2\left(\frac{4\pi h_t h_{\mathrm{Rx}}}{\lambda d}\right). \tag{3}$$

3) *Desirability of a Comprehensive Model:* Although it is possible to model the performance using the two limiting cases considered above, it is actually better to create a more comprehensive model that can calculate the effects of the multipath in any geometry and in any conditions of sea state and signal polarization and can automatically take these into account. This means that the modeler does not have to make a judgment at each stage as to which limiting condition best approximates the actual scenario. The modeling used to predict the performance of the system proposed here, therefore, automatically took account of the roughness of the sea [11] and of the variation of the effective reflection coefficient with grazing angle and polarization [12]. It also uses a "spherical" earth model for the sea surface when finding the reflection point of the rays.

D. Modeling the Backscatter from the Sea

As soon as the wave heights (expressed by the Douglas sea state [13]) become significant, the backscatter from the sea also becomes significant. The power scattered from the sea surface and received by the radar is given by

$$P_{cl} = \frac{P_{\mathrm{FD}} \sigma^0 A_{\mathrm{cell}}\, A_{\mathrm{Rx}}}{4\pi d^2} \tag{4}$$

where PFD is the PFD in the vicinity of a target area, Acell is the footprint of the sea surface reflecting into a single receiver resolution cell and σ^0 is the RCS per unit area of the sea surface area, which depends on the sea state, the grazing angle, and the frequency and polarization of the radar signals.

The resolution cell area Acell can be approximated as

$$A_{\mathrm{cell}} = \Delta R \cdot \Delta\theta \cdot d \tag{5}$$

where

$$\Delta R = \frac{c}{2B_{\mathrm{sig}}} \tag{6}$$

is the range resolution, Bsig is the transmitted signal bandwidth, c is the speed of light, and $\Delta\theta$ is the angular resolution expressed in radians, which can be approximated by the one-way 3 dB beamwidth of the receiver antenna.

E. Signal to Noise

The most general way to calculate the sensitivity of the radar is to use the mean power level of the signals, which is in accord with the consequence of the matched filter theorem [14] that the sensitivity of radar is determined by its mean power rather than its peak power.

This approach avoids the need to consider pulse compression gain or any details of the waveform (such as its bandwidth) in the calculations. The received signal level is then compared to the noise floor to determine the sensitivity of the radar. The most appropriate bandwidth to use when determining the sensitivity is the data rate at which the radar must pass information to whatever system is to use that information, since this limits the possible integration time. This is equivalent to the approach used to determine the "surveillance radar range equation" [15].

At its most basic, this approach, therefore, determines the sensitivity based on the energy received from the target (mean power times integration time, which is equivalent to mean power divided by bandwidth). The basic equation according to this scheme gives the best attainable performance because it assumes the perfect integration of the received signals. Losses due to practical implementation considerations, such as mismatching of the filtering to reduce sidelobes or the need to use incoherent integration and other losses due to other imperfections in the system, can then be incorporated as required.

The receiver noise power is given as

$$N = kTBN_r \tag{7}$$

where kT is the product of Boltzmann's constant and the temperature, N_r is the receiver noise factor, and B is the reciprocal of the integration time.

It is important to distinguish between the signal bandwidth in (6), and the noise bandwidth used in (7).

If we do not need to consider noise from external sources, such as atmospheric noise, using (7), the free space SNR ratio is then given as

$$\mathrm{SNR}^{\mathrm{FS}} = \frac{P_{\mathrm{FD}} A_{\mathrm{Rx}} \sigma}{4\pi d^2 kTBN}. \tag{8}$$

F. Clutter to Noise

The final calculation of the radar performance needs to take into account the effects of clutter as well as noise. By comparing the clutter to noise ratio (CNR) and the SNR it becomes easy to identify the two limiting cases, the first when the clutter is negligible and the sensitivity is limited by the receiver noise and the second where the clutter is dominant.

The CNR can be calculated by (4) and (7), and is given as

$$\mathrm{CNR} = \frac{P_{\mathrm{FD}} \sigma^0 A_{\mathrm{cell}}\ A_{\mathrm{Rx}}}{4\pi d^2 kTBN}. \tag{9}$$

There is relatively little data on the specific RCS of sea clutter in bistatic geometries. The data suggest that the bistatic values are on average slightly lower than the monostatic, but the differences are small and in view of the lack of data, the modeling performed here uses monostatic values, although these may be slightly conservative.

In practical calculations, discussed in the next section, we will use values for σ_0 based largely on the experimentally measured values tabulated in [16]. Several attempts have been made to parameterize this dataset in order to refine the estimates at the spot frequencies and a smoothing scheme is being used in our calculations, which was created at the Royal Radar Establishment, as it then was, in the U.K. This work of parameterizing the values is described in [17]. Similar parameters to those described in [17] of the X-band also exist for the L-band frequencies used here. Using this parameterization is another decision that is probably conservative since this model predicts significantly higher levels of backscatter at low grazing angles compared to some other models, such as that described in [18].

The experimental data values in [16] exist for specific (integral) values of the sea state, for specific (nominal) frequencies, and specific grazing angles and the software interpolates between these values.

Data exist for horizontal and vertical polarizations. Very little actual data exist for circular polarization, even for monostatic scenarios. The general assumption is that the values for circular polarization are the "average" of those for the two linear polarizations. In fact, such an assumption, particularly when applied equally to both co- and cross-circular polarizations, implies some unlikely relative phase behavior between the different linearly polarized components. This modeling, therefore, used the vertically polarized data as a worst case, i.e., once again it took a conservative approach.

G. Assumptions

As explained above, the receiver bandwidth is assumed to be the reciprocal of the data update rate, which may be of the order of 24/min for a marine radar, giving an integration time of 2.5 s.

Where multiple transmitters are available, the effective power density has been used based on the assumption that the signals can be integrated together incoherently. In [19], typical curves for an incoherent integration gain can be found. Many authors agree that for the radar case, with relatively high SNR and relatively small numbers of uncorrelated samples (≤ 1000), these curves can be parameterized by a gain of n^k, where n is the number of samples and the exponent k is less than 1. For the modeling shown here the parametrization is $n^{3/4}$, which the authors believe to be the best model. Therefore, in this case, if n equal-power transmitters are available, each of power density P_0 at the target, the total effective power density can be taken as $P_0 n^{3/4}$. With four effective samples integrated, the gain will thus be about 5 dB rather than the ideal value of 6 dB. The effective flux density will be -73 dBm/m^2.

Combining four channels that are close together and each of which have a bandwidth of 200 kHz will typically give a system bandwidth of 0.8 MHz [20] so the radial length of the clutter cell can be taken to be 188 m.

In order to find the difference in the lengths of the direct and indirect paths, the multipath model has to find the point where the multipath ray over a spherical earth is reflected from the sea surface. This is done by an iterative method. The multipath model is applied to the signal scattered from

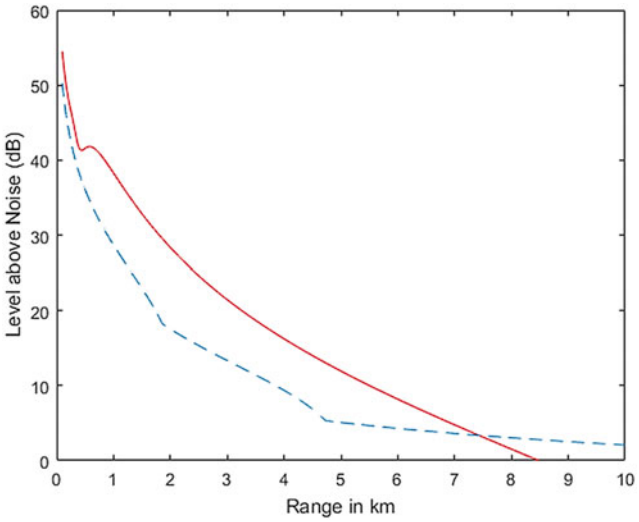

Fig. 2. SNR (solid red) and CNR (dotted blue) for 10 m^2 target at 3.5 m height in Sea State 5.

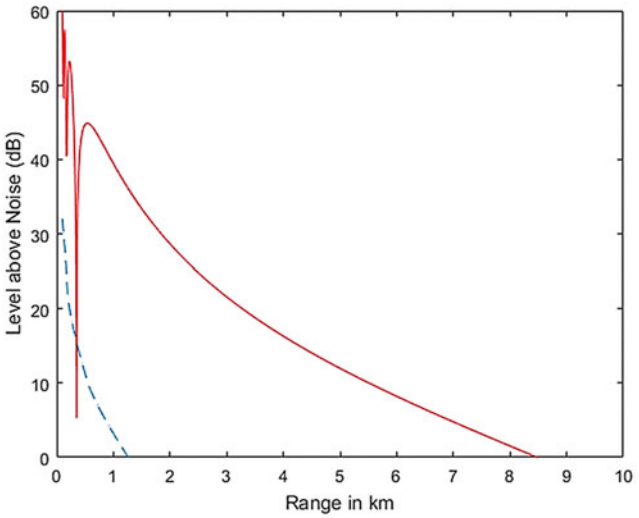

Fig. 3. Corresponding data for the opposite extreme, Sea State 0.

the target to the receiver. It is assumed that the elevation angle of the transmitter from the target will be high enough that the effects of multipath on the signal travelling from the transmitter to the target can be ignored.

A value of 2 dB may be taken for the noise figure. This is the same as that obtained for the experimental receiver discussed in Section IV.

The receiver aperture will be taken as -8 dBm^2. This corresponds to a pencil beam with a width of about 26°, which is appropriate to give a wide enough field of view to see objects that might pose a hazard to the boat. A relatively wide elevation beamwidth is needed to accommodate pitching of the boat.

H. Modeling Results

Fig. 2 shows the SNR, the red line, the CNR, and the blue line.

The curves show the total sea clutter return. If operation is required in sea state 5, it should be noted that the

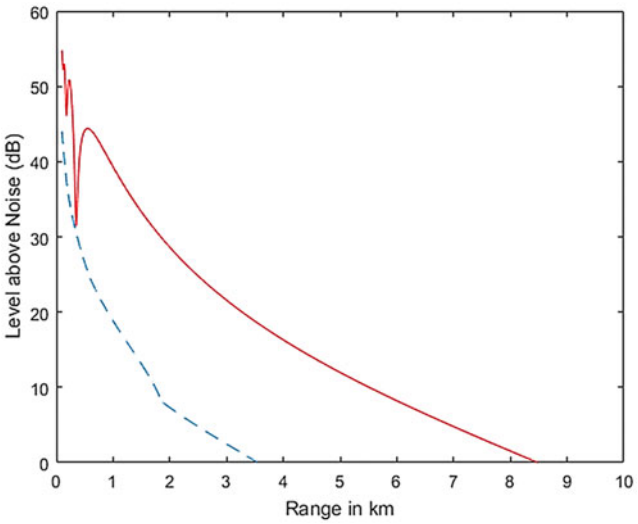

Fig. 4. SNR (Upper Curve) and CNR (Lower Curve) for 10 m^2 target in Sea State 3.

signal-to-clutter ratio can be improved by at least 10 dB by the coherent processing since the clutter will be spread over about 20 Hz spectral width but the target will be concentrated in a single velocity bin. The motion of the boat will also further spread the clutter spectrum due to Doppler beam sharpening [21], so a useable signal-to-clutter ratio should also be obtainable even in this sea state.

Here, as expected, the clutter levels are very low and the performance is noise limited. Although the general performance is much better, there are deep nulls at shorter ranges due to the effects of multipath. These effects are much more severe with the lower sea state because the reflections are more coherent and hence the cancellation at the multipath nulls is deeper.

For completeness, Fig. 4 shows the behavior in the intermediate case of sea state 3.

IV. VERIfiCATION OF THE SENSITIVITY CALCULATIONS

A measurement campaign to confirm the power budgets was undertaken. As this took place within the United Kingdom, it used the ALPHASAT (INMARSAT 4A-F4 25E) satellite as the emitter. It also used a coherent combination of four signal channels to provide an overall signal bandwidth of 0.8 MHz [21] that reduced the size of the clutter patch, and hence improved the clutter levels compared to those assumed in the calculations for the final system.

The trials used to confirm the sensitivity calculations were conducted during summer–autumn of 2015 with the radar at Constitution Hill, Aberystwyth, Wales, U.K. (52°25'30.78"N, 4°0.5'02.26"W). The receiver site was 100 m above sea level.

A Google Earth photograph of the site, radar configuration, and trajectories of a target recorded by GPS logger are shown in Fig. 5.

During trials, the boat, which was 10.5 m long, [see Fig. 5(b)], was used as a cooperative target. Its displacement is 9.5 tons, and using a common rule of thumb equating the

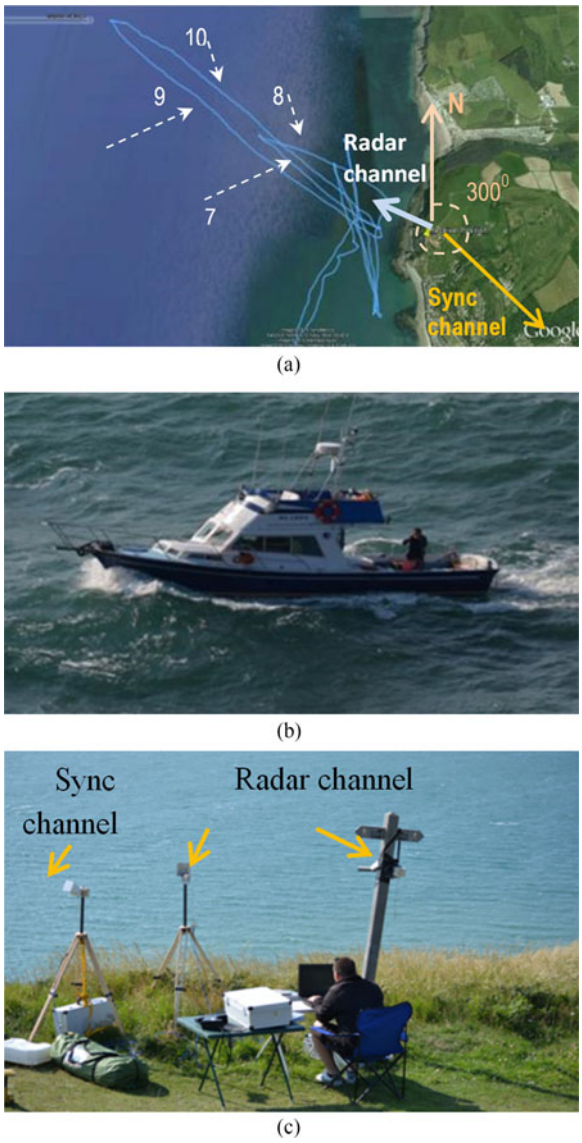

Fig. 5. (a) Google Earth photo with marked location of the receiving equipment, radar, and sync antennas directions and boat tracks during the experiments, recorded through its onboard GPS logger; (b) target; (c) receiver antennas.

RCS in square meters to the displacement in tons [22], certainly at moderate grazing angles we would expect that the monostatic RCS of the boat is about 10 dBm^2. The boat was moving with two speeds: "high" of 9–10 knots when moving with the seas and "low" of about 6 knots when moving against seas.

A medium specification GPS data logger of 1 s update rate was onboard the boat to record its positions and velocities.

Two boat trajectories were of particular interest to establish measured range and Doppler resolution: normal to and parallel to the line of sight to the radar antenna.

The sea state could be estimated from the weather buoy data that can be downloaded from the Internet [23]. The nearest buoy was just off Aberporth, about 25 mi down the coast. During the period of the trials, the wind speed was between 10 and 11 kts, approximately from the North. The wave height was between about 2 and 2.5 ft. This corresponds to a Douglas sea state on the border between sea state 2 and sea state 3.

Due to relatively high sea state, boat trajectories were chosen to be not exactly parallel or perpendicular to the coast line, but at an angle, as shown in Fig. 5(a). The course had to be adjusted according to wind and wave direction and severity.

The sync antenna was invariably directed to the satellite that has an elevation of about 26° above the horizon and with radar antenna looking into the sea they defined nearly monostatic geometry of satellite–target–receiver and nearly ideal radial direction of the boat moving along trajectories 7–10, as shown in Fig. 5(a).

The receiver was based on NI USRP (Universal Software Radio Peripheral) type USRP-2950R. The settings of the USRP and parameters used for signal acquisition are given in Table II.

The overall noise figure of the radar receiver channel is about 2 dB.

Fig. 6 shows a set of several consecutive range-Doppler frames as well as amplitude range-Doppler surfaces of total 120 s record of the boat moving along the trajectory 9 [see Fig. 5(a)].

The frames here are defined as range-Doppler maps of sections of signal starting at consecutive times were integrated over 1 s coherently and then over 10 s noncoherently. The conventional "long integration time" processing and "bands stitching" procedures were used, as described in [3] and [20]. As reported in [20], the examination of the characteristics of the signals suggests that it is routinely possible to find groups of adjacent, or nearly adjacent channels that can be combined in this way.

In each frame, there is an area of elevated signal amplitudes within positive Doppler bins encompassing 0–20 Hz, which relates to an inshore sea clutter. Indeed, in case of incoming seas to the coast (as for data collected), it produces positive Doppler shift around of 10 Hz as well defined swells travel with a speed of around of 1 m/s. There will be some outward weaker backward waves after bouncing to the shore which rapidly attenuates, so that close to the shoreline the Doppler shift is expected to have a small component with the opposite sign that again explain the spread in negative Doppler domain area. The strongest sea reflections are visible at short range which is a minimum range of antenna beam footprint on the sea surface, i.e., at the second range cell from the receiver. Then, it extends along the range with the appropriate reduction of reflected power with the distance.

The reflection from a boat is seen as a blob (in dashed circle) appearing in consecutive range resolution cells in successive frames and around −40 Hz Doppler, which would be the nearly monostatic Doppler shift corresponding to a target outward radial speed of 5 m/s. The progression of the boat in cells for series frames (see Table III) indicates an agreement with the speed estimated from Doppler shift as over each 30 s it passes into the next resolution cell. The boat GPS data confirm these results and correspondingly

TABLE II
Receiver Parameters

	Sync Channel	Radar Channel
USRP reference frequency source	GPSDO	
USRP LNA gain	+30 dB	+30 dB
USRP acquisition centre frequency	1.5534 GHz	1.5534 GHz
USRP I/Q dampling rate	2 MHz	2 MHz
Antenna	Horn: (2 dBi Gain)	Helical: Gain 16 dBi)
Front-End LNA	None	Minicircuits ZEL-12126-LN, 23 dB Gain, 1.5 dB noise figure
Antenna direction	Stared at expected Azimuth 26° East, Elevation 29°	300° azimuth −10° elevation

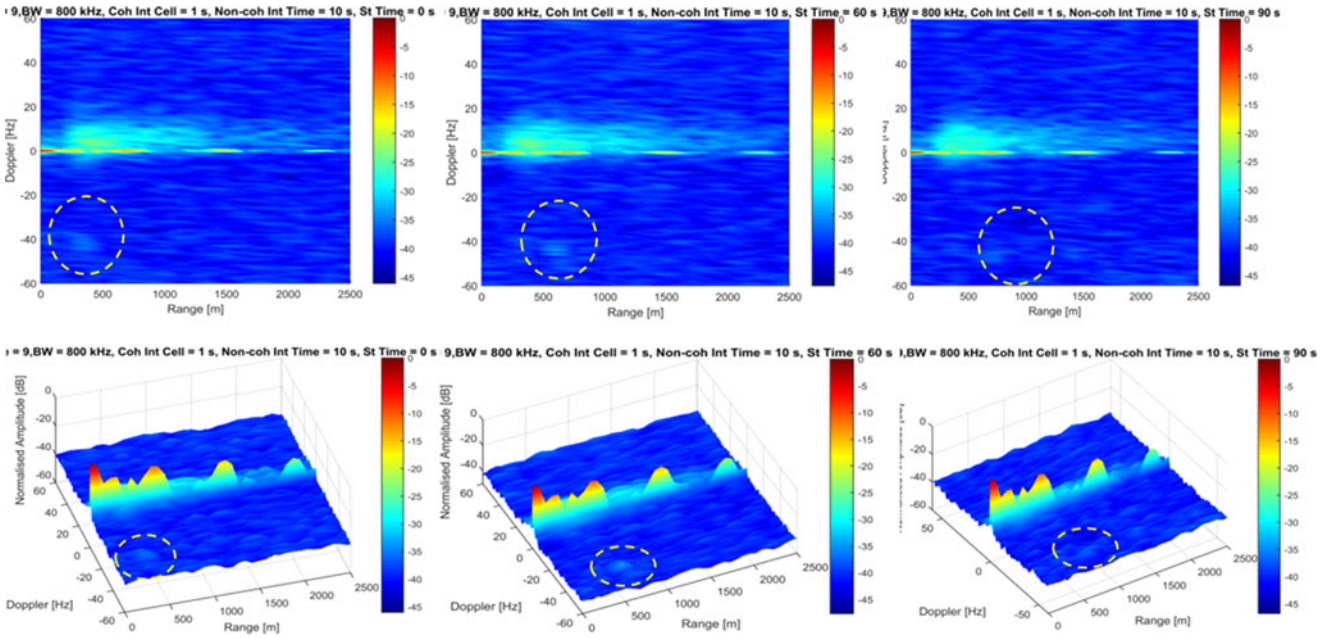

Fig. 6. Range-Doppler maps of the boat moving radially out by trajectory 9 of Fig. 5(a).

TABLE III
Target Position Versus Time

Frame	Start Time (s)	Approximate Range (m)
1	0	300
2	30	450
3	60	600
4	90	750
5	120	900

confirms that the boat has been correctly identified in the range-Doppler plots.

V. COMPARISON OF THEORY AND EXPERIMENT

Although the target in the experimental scenario was at relatively short range and the radar height was significantly higher than for the proposed applications, the same modeling tools are applicable to both environments so the experimental data can be used to validate the modeling discussed in Section III. Fig 7 shows the predicted performance of the radar.

It can be seen that in this geometry, the signal-to-clutter ratio is quite poor at short ranges due to the high depression angle. The expected SNR for this scenario with the target at 500 m range is 33 dB. This is lower than that might be expected from the data in Figs. 2–4 because the integration time in the experiments was only 1 s. The modeling predicts that the CNR in this scenario would be −1 dB.

A. SNR Ratio

From Fig. 6, the background level is about −40 dB and the signal level is about 5 dB above this. The target is, however, spread over about 10 Hz in Doppler, which implies that the total power received from it is 10 dB higher than that seen in a single Doppler bin, so the signal-to-background ratio for an equivalent point target, where all the energy would be concentrated into a single range-Doppler

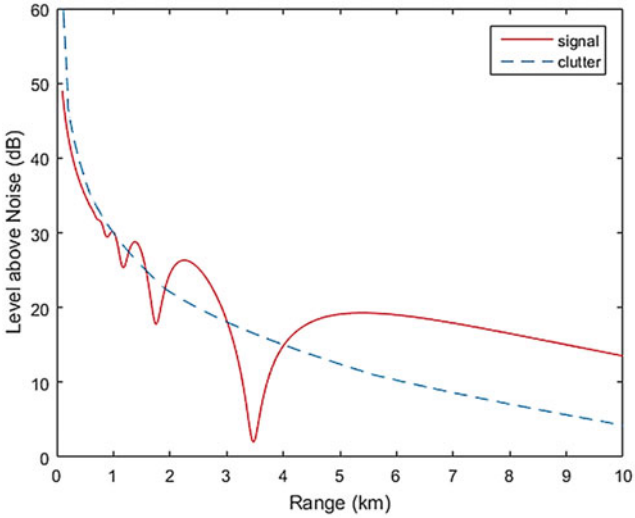

Fig. 7. SNR (Upper Curve) and CNR (Lower Curve) for 10 m^2 target in Sea State 3—100-m radar altitude.

bin, would be about 15 dB. In fact, the background level is about 9 dB above the noise floor because it is dominated by the sidelobes from close-in targets. This effect could easily be reduced in a real system by partially nulling the direct signal. The SNR for an equivalent point target would thus be 24 dB.

The apparent discrepancy between the expected and observed sensitivity is best attributed to the fact that the bistatic RCS of a man-made target will be expected to be lower than the monostatic value because of the major contribution that corner reflectors make to the monostatic RCS. No similar structures, which would have to produce strong scattering from transmitter to receiver over a wide range of geometries, can be expected in the general bistatic case. The reduction of 9 dB (i.e., a bistatic RCS of about 1.2 m^2 compared to an expected monostatic RCS of 10 m^2) is very significant, but not implausible. The simulations of bistatic RCS of ships, which are discussed in [24], also support the hypothesis that one should expect significantly lower RCS values in bistatic geometries.

B. Clutter Level

The clutter level is about 5 dB higher than the signal, and spread over perhaps 30% more of spectrum than the target. The signal-to-clutter ratio is thus about −6 dB.

If the signal level is 9 dB lower than expected, this suggests that the clutter level is 4 dB less than that would be expected from the monostatic data. This could be seen as supporting other work [25], which suggests that the bistatic clutter RCS is generally lower than the monostatic, but the inaccuracies associated both with the number of parameters that have had to be estimated to deduce the RCS values and with inherent variability of sea clutter levels mean that this data can provide only very limited support to that thesis.

VI. CONCLUSION

The viability of systems has been demonstrated for pervasive global surveillance by bistatic radars using satellite communication systems as illuminators. The use of Inmarsat signals as illuminators has been explored. A simple marine obstacle avoidance system has been outlined as an example application. The SNR ratio is strongly affected by multipath, particularly so at lower sea states, and at high sea states the sensitivity is likely to be limited by sea clutter. Despite these factors, good SNR and signal-to-clutter ratios are predicted for ranges of up to about 5 km over the whole range of sea states.

The modeling behind these predictions has been verified by an experiment.

The comparison of the predictions and the measurements has shown that the clutter levels are very much as would be expected, i.e., slightly below the expected monostatic values, but the bistatic RCS of a small ship is shown to be about 9 dB below the expected monostatic value. The reduced bistatic RCS does not invalidate the practicality of the proposed system, but does have to be taken into account when predicting the performance of bistatic systems.

REFERENCES

[1] H. D. Griffiths and C. J. Baker
An Introduction to Passive Radar. Norwood, MA, USA: Artech House, 2017

[2] D. Cristallini *et al.*
Space-based passive radar enabled by the new generation of geostationary broadcast satellites
in *Proc. IEEE Aerosp. Conf.*, Mar. 2010, pp. 1–11.

[3] P. E. Howland, D. Maksimiuk, and G. Reitsma
FM radio based bistatic radar
IEE Proc., Radar, Sonar Navig., vol. 152, no. 3, pp. 107–115, Jun. 2005.

[4] H. D. Griffiths and C. J. Baker
Passive coherent location radar systems. Part 1: Performance prediction
IEE Proc., Radar, Sonar Navig., vol. 152, no. 3, pp. 153–159, Jun. 2005.

[5] F. Colone, D. W. O'Hagan, P. Lombardo, and C. J. Baker
A multistage processing algorithm for disturbance removal and target detection in passive bistatic radar
IEEE Trans. Aerosp. Electron. Syst., vol. 45, no. 2, pp. 698–722, Apr. 2009.

[6] D. Poullin
Passive detection using digital broadcasters (DAB, DVB) with COFDM modulation
IEE Proc., Radar, Sonar and Navig., vol. 152, no. 3, pp. 143–152, Jun. 2005.

[7] *Detailed Specifications of the Radio Interfaces for the Satellite Component of International Mobile Telecommunications*, ITU Recommendation ITU-R M.1850-1, Dec. 2012, Section 4.3.4.1, Table 25

[8] [Online]. Available: http://www.bundesnetzagentur.de/EN/Areas/Telecommunications/Companies/FrequencyManagement/FrequencyAssignment/SatelliteCommunications/Inmarsat Basepage.html, Accessed on: Jul. 28, 2016.

[9] *Maritime Navigation and Radiocommunication Equipment and Systems Radar Part 1: Ship Borne Radar Performance Requirements Methods of Testing and Required Test Results*, IEC 60926-1, 1998, Section 3.3.2.

[10] J. N. Briggs
Target Detection by Marine Radar, (ser. Radar, Sonar, Navigation and Avionics). Stevenage, U.K: Inst.Eng. Technol., 2004. [Online]. Available: http://digital-library.theiet.org/content/books/ ra/pbra016e

[11] F. Nathanson
Radar Design Principles: Signal Processing and the Environment. New York, NY, USA: McGraw-Hill, 1969 [Sea Roughness].
[12] M. Skolnik
Introduction to Radar Systems, (Electrical engineering series). New York, NY, USA: McGraw Hill, 2001 [Reflection Coefficients].
[13] F. Nathanson
Radar Design Principles: Signal Processing and the Environment. New York, NY, USA: McGraw-Hill, 1969 [Reference to Douglas Sea State].
[14] C. Cook and M. Bernfeld
Radar Signals: An Introduction to Theory and Application (Electrical Science Series). New York, NY, USA: Academic, 1967, ch. 2.
[15] M. Skolnik
Introduction to Radar Systems (ser. Electrical engineering series). New York, NY, USA: McGraw Hill, 2001 [Eq. 2.63].
[16] F. Nathanson
Radar Design Principles: Signal Processing and the Environment, New York, NY, USA: McGraw-Hill, 1969 [Sea Clutter Data].
[17] K. Ward, R. Tough, and S. Watts
Sea Clutter: Scattering, the K Distribution and Radar Performance (IET Radar, Sonar, Navigation and Avionics Series). Stevenage, U.K.: Inst. Eng. Technol., 2006 [Section 8.3].
[18] M. M. Horst, F. B. Dyer, and M. T. Tuley
Radar sea clutter model
in *Proc. Int. Conf. Antennas Propag.*, 1978, pp. 6–10.
[19] M. Skolnik
Introduction to Radar Systems (ser. Electrical engineering series). New York, NY, USA: McGraw-Hill, 2001 [Fig. 2.7]
[20] X. Lyu, A. Stove, M. Gashinova, and M. Cherniakov
Ambiguity function of inmarsat BGAN signal for radar application
Electron. Lett, vol. 52, no. 18, pp. 1557–1559, Sep. 2, 2016.
[21] M. Skolnik
Introduction to Radar Systems (ser. Electrical Engineering Series). New York, NY, USA: McGraw Hill, 2001, pp. 21.5–21.6.
[22] M. Skolnik
Introduction to Radar Systems (ser. Electrical Engineering Series). New York, NY, USA: McGraw-Hill, 2001 [Table 2.1].
[23] [Online]. Available: http://www.ndbc.noaa.gov/maps/United Kingdom.shtml, Accessed on: Oct. 2015.
[24] M. Gashinova, L. Daniel, S. Hristov, X. Lyu, A. G. Stove, and M. Cherniakov
Passive Radar for Ship Detection using Communication Satellite Signals
IEEE Trans, Aerospace & Electron. Syst.
[25] H. D. Griffiths, W. A. Al-Ashwal, K. D. Ward, R. J. A. Tough, C. J. Baker, and K. Woodbridge
Measurement and modelling of bistatic clutter
IET Radar, Sonar Navig., vol. 4, no. 2, pp. 280–292, Apr. 2010.

Andrew G. Stove (M'98–SM'04) received the B.A. degree in engineering science and the D.Phil degree for work on surface acoustic wave devices from Oxford University, Oxford, U.K., in 1977 and 1981, respectively.

In 1980, he joined the Philips Research Laboratories, Redhill, U.K., where he worked on frequency modulated continuous wave (FMCW) radar systems with applications in smart ammunition, automotive radar, and low probability of intercept marine navigation. During that period, he was also involved in three bistatic radar projects. In 1996, he joined the Racal Radar Defence Systems, which is now a part of Thales, where he worked on the design for the Searchwater 2000 radar family and on the analysis of the subsequent trials data, including improving the understanding of the behavior of the sea clutter. Other activities include work on radar target classification and bistatic radar research. He was the Industry Co-Chair of the UK's Radar Tower of Excellence. He was also the Co-Chairman of the NATO SET-184 Noise Radar Group and is currently the Co-Chairman of its successor group. In 2015, he left Thales and is currently an Honorary Professor at the University of Birmingham, Birmingham, U.K., and a Visiting Professor at the University College London, London, U.K. He has also been an Alan Tayler Visiting Lecturer in applied mathematics at the University of Oxford.

Dr. Stove a Fellow of the Institution of Engineering and Technology (the successor of the Institution of Electrical Engineers).

Marina S. Gashinova received the M.Sc. degree in math from St-Petersburg State University, Saint Petersburg, Russia, in 1991, and the Ph.D. degree in physics and math from St-Petersburg Electrotechnical University, Saint Petersburg, Russia, in 2003.

In 2006, she joined the Microwave Integrated System Laboratory, University of Birmingham, where she is currently a Senior Lecturer in radar and RF sensors, leading the research group on passive and active bistatic radar, THz radar imaging and automotive sensors. She is an author/coauthor of more than 80 publications in peer-reviewed journals and conferences' proceedings and presenter of several invited and focused talks on forward scatter radar at international conferences, workshops, and seminars.

Stanislav Hristov received the B.Sc. degree in physics with particle physics and cosmology in 2012 from the University of Birmingham, Birmingham, U.K, where he has been working toward the Ph.D. degree in electrical, electronic and systems engineering since 2012.

His main research interests include software-defined hardware systems, passive radars and target imaging, and classification in forward scatter radar (FSR).

Mikhail Cherniakov received the Graduate in electronics, Ph.D. degree in microwave systems, and D.Sc. degree from Moscow Technical University, Moscow, Russia, in 1974, 1980, and 1992, respectively.

He was a Full Professor at the Moscow Technical University in 1993. In 1994, he was a Visiting Professor at the University of Cambridge, and in 1995, he moved to the University of Queensland, Australia. In 2000, he joined the School of Electronic, Electrical and Systems Engineering, Birmingham, U.K., where he founded the Microwave Integrated Systems Laboratory that is the biggest radar research team in U.K. Universities. He is the author/editor/coauthor of 3 books, and has more than 250 peer-reviewed publications. He is the Chair in Aerospace and Electronic Systems, University of Birmingham, Birmingham, U.K., with more than 40 years' experience on the R&D in radar systems. His research interests include bistatic and multistatic radar, radars with phased array, automotive, and short-range sensors.